Chinese Chemical Letters 33 (2022) 3488–3491

Contents lists available at ScienceDirect

Chinese Chemical Letters

journal homepage: www.elsevier.com/locate/cclet

Broken electron transfer pathway in enzyme: Gold clusters inhibiting TrxR1/Trx *via* cell studies and theory simulations

Wenchao Niu[a,b], Zhongying Du[a], Chunyu Zhang[a], Deting Xu[b,c], Jiaojiao Li[a], Minghui Sun[b,c], Liyuan Wu[b], Haodong Yao[b], Lina Zhao[b,c,*], Xueyun Gao[a,*]

[a] *Department of Chemistry and Biology, Beijing University of Technology, Beijing 100124, China*
[b] *CAS Key Laboratory for Biomedical Effects of Nanomaterials and Nanosafety, Institute of High Energy Physics, Chinese Academy of Sciences, Beijing 100049, China*
[c] *University of Chinese Academy of Sciences, Beijing 100049, China*

ARTICLE INFO

Article history:
Received 28 January 2022
Revised 1 April 2022
Accepted 1 April 2022
Available online 5 April 2022

Keywords:
Enzyme inhibition
Electron transfer
Thioredoxin reductase 1
Gold clusters
Molecular dynamics
Density functional theory

ABSTRACT

Thioredoxin reductase 1 (TrxR1) is over activity in tumor cell to maintain their redox balance. Although gold clusters have great potential in antitumor drug as they could well inhibit TrxR1, the molecular mechanism has not been disclosed yet. In this work, we revealed gold clusters can well inhibit the activity of TrxR1 in lung tumor cells and further disclosed the inhibition mechanism by using computational simulation methods. We firstly inferred the binding sites of gold in the hydrophobic cavities on TrxR1. The simulation results show that the gold ion (released from Au cluster) interact with –SH of Cys189 in TrxR1, this greatly increase the distance between the C-terminal redox center of TrxR1 and the Trx redox center, thereby destroy the electron transfer pathway between them. Our electron transfer destroying mechanism is different from the previous hypothesis that gold binds to the Sec498 of TrxR1 which has never been proved by experimental and theory studies. This work provides a new understanding of the gold clusters to inhibit TrxR1 activity.

The redox system composed of thioredoxin reductase (TrxR) and thioredoxin (Trx) is an important part of maintaining the redox balance of organisms, and plays a key role in regulating cell growth, differentiation, and death [1]. TrxR is overactivated in most cancer cells and is a specific target for anticancer drugs [2,3]. The cytoplasmic type (TrxR1) [4] is the earliest discovered, widely distributed, and one of the most studied thioredoxin proteases [5,6]. Many inhibitors have been developed to inhibit the activity of TrxR1, including platinum complexes [7], gold compounds [8,9], selenium compounds [10,11], *etc*. The affinity of gold and –SH group plays a key role in the process of inhibiting TrxR1 activity [12]. However, the mechanism of inhibiting TrxR1 enzyme activity is still unclear, and there are still no clinical anticancer drugs that target the TrxR1/Trx system well.

The crystal structure of TrxR1 clearly shows that the C-terminal redox center (Cys497/Sec498) is located on the surface of TrxR1 [13]. It provides a structural basis for selectively targeting C-terminal redox sites. In fact, most of the current TrxR1 inhibitors are electrophiles or nucleophiles, and inhibit enzyme activity by binding to the enzyme's surface exposure and highly reactive selenocysteine [14]. However, there are also reports with very different viewpoints confirming that the gold ion binding position may not be the expected C-terminal redox site (Cys497/Sec498). Parsonage *et al*. reported that in the crystal structure of auranofin co-incubated with TrxR, the only modified residue of gold ion is not the redox center of *Entamoeba histolytica* TrxR [15]. Angelucci *et al*. reported that gold compounds release gold ions, which modify only cysteine residues of *Schistosoma mansoni* enzyme [16]. In addition, Fritz-Wolf *et al*. reported the structural details of the human TrxR1/Trx complex. The contact surface of the TrxR1/Trx complex is small, including only weak interactions Trp31-Trp114′, Lys36-Glu103′, Asp60-Arg117′, Asp63-Lys146′, Glu70-Arg121′ and Lys72-Glu122′ [17]. In other words, the combination between TrxR1 and Trx is very sensitive and easily interfered or destroyed by chemical inhibitors.

In recent years, due to the unique chemical properties and good biocompatibility, gold clusters have received great attention and made great progress in cancer cell targeting and treatment [18–21]. Gao group has constructed a gold cluster molecule that emits blue fluorescence, which can specifically label the cell membrane epidermal growth factor receptor (EGFR) [22]. In addition, Gao *et al*.

* Corresponding authors.
E-mail addresses: linazhao@ihep.ac.cn (L. Zhao), gaoxy@ihep.ac.cn (X. Gao).

https://doi.org/10.1016/j.cclet.2022.04.004
1001-8417/

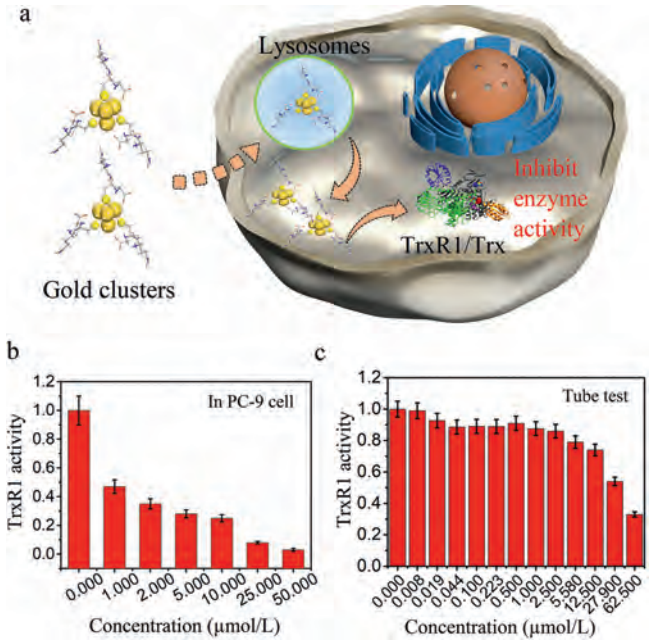

Fig. 1. The activity of TrxR1 is inhibited by gold clusters. (a) Schematic illustration of the Au clusters inhibiting TrxR1 enzyme activity in cell. (b) TrxR1 activity measured after co-incubation of gold clusters with different concentrations of PC-9 cells. (c) The TrxR1 enzyme activity measured after co-incubation of a series of the gold clusters in tube.

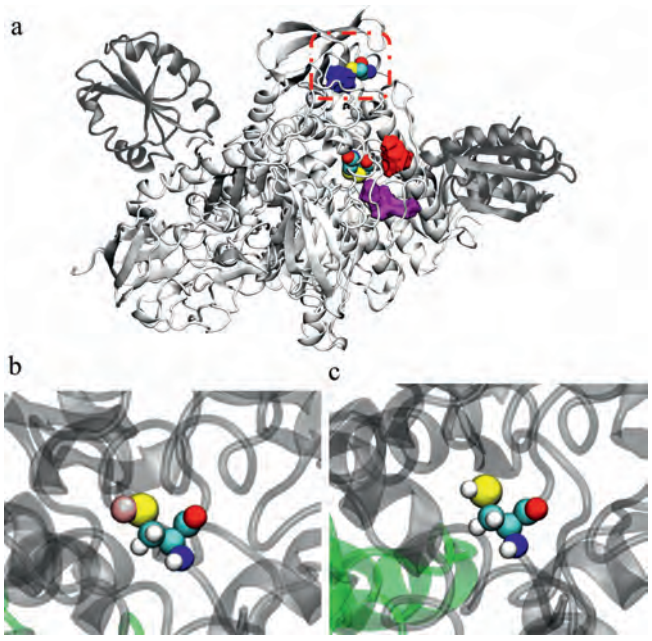

Fig. 2. Building the structures of the simulation systems. (a) The distribution of the hydrophobic cavities near the α-helix that interacts with Trx as the hydrophobic cavity A (purple), B (red) and C (blue). The Cys59/Cys64 of the N-terminal redox center and the starting position of the α-helix Cys189 are all marked with van der Waals representation. The red dashed line denotes the surrounding of Cys189. (b) The Cys189-Au interaction (Sys-1). (c) The Cys189 residue (Sys-2).

found that gold clusters can effectively inhibit TrxR1 in the cytoplasm of tumor cells. They observed that gold clusters significantly inhibit TrxR1 activity in the cytoplasm, induce an up-regulation of activated PARP levels, and cause tumor cell apoptosis [23]. However, until now, the mechanism of how gold clusters inhibit the activity of TrxR1 is still a topic without clear picture.

We synthesized a type of gold clusters (Details can be found in Supporting information) [24]. After the gold clusters were uptake into the cells, we examined the effect of gold clusters on the enzyme activity of TrxR1 in PC-9 cell, as shown in Fig. 1a. PC-9 cells were incubated with a series of gold clusters doses. After extracting the whole cell protein, the intracellular TrxR1 activities were determined by a TrxR1 activity assay. From the result of Fig. 1b, the activity of TrxR1 was effectively suppressed by the gold clusters in dose dependent manner. Meanwhile, the purified TrxR1 protein was directly incubated with a series of gold clusters in tube, and the TrxR1 enzyme activity was also inhibited obviously, as shown in Fig. 1c. From the above results, we could conclude that the gold clusters have a certain inhibitory effect on TrxR1 enzyme activity.

It is well known that hydrophobic cavities in proteins are beneficial to the combination of small molecules, gold clusters and other ions. According to the crystal structure of TrxR1 in combination of TrxR1/Trx (3QFB), the distribution of all hydrophobic cavities is statistically analyzed. It was found that there are three hydrophobic cavities near the α-helix bound to Trx in TrxR1, as shown in Fig. 2a. The hydrophobic cavity A (purple) is located between the C-terminal redox center and the N-terminal redox center near the C terminal with a volume as 235 Å^3. The hydrophobic cavity B (red) is composed of the α-helix of TrxR1, the C-terminus of the other monomer and some amino acids of the substrate Trx with a volume as 192 Å^3. The formations of these two hydrophobic cavities are affected by the swing of the C terminal. When the C-terminal (Cys497/Sec498) of TrxR1 obtains an electron from the N-terminal redox center, it will extend into the hydrophobic cavity A. After obtaining the electron, it will extend to the solution, and the hydrophobic cavity B will be formed when the substrate is ready to be reduced [25]. The hydrophobic cavity C (blue) is located at the starting position of the α-helix that interacts with the substrate with a volume as 114 Å^3. It is the smallest one among these three hydrophobic cavities, while this region is located on the surface of TrxR1, which is beneficial to interact with different inhibitors (such as gold clusters). The most important thing is this hydrophobic cavity includes cysteine, which can be well anchored by gold ions. Recently, more and more evidence has shown that when gold clusters enter the living body and after the metabolism, gold ions are released and anchored to the sulfur atoms on cysteine [26,27]. Here, we constructed TrxR1/Trx simulation structures with (Sys-1) or without (Sys-2) gold ion respectively (Figs. 2b and c).

In Sys-1 model (Fig. 2b), the selenium atom in selenocysteine is activated, which corresponds to the process that the C-terminal Sec498 of TrxR1 obtains electrons and is ready to be delivered to the substrate Trx. In order to observe the possible changes caused by the gold ions, we restored the mutated amino acid to the wild type and the C-terminus to Sec498 based on the crystal structure data of 3QFB. The constructed TrxR1/Trx wild-type Sys-2 structure model (Fig. 2c) was used as a control system, and then molecular dynamics simulations were performed on Sys-1 and Sys-2 to learn their dynamics behaviors.

The Sys-1 reached a steady state after 90 ns run. Its average root mean square deviation (RMSD) of protein backbone was 2.9 Å in the range of 90–120 ns simulation. The Sys-2 system describes the wild-type TrxR1/Trx system, which has been in a stable state since the 20th ns. Its average RMSD of protein backbone was 2.7 Å during the equilibrium period as 90–120 ns as shown in Fig. S2a (Supporting information). We used newly generated force field parameters to calculate Sec498 as shown in Fig. S1 (Supporting information). In Sys-2, the geometric structure of Sec498 remains stable, reproducing the state where the C-terminal redox center of TrxR1 in the crystal structure is in contact with the redox center of Trx, indicating that the newly generated force field parameters are

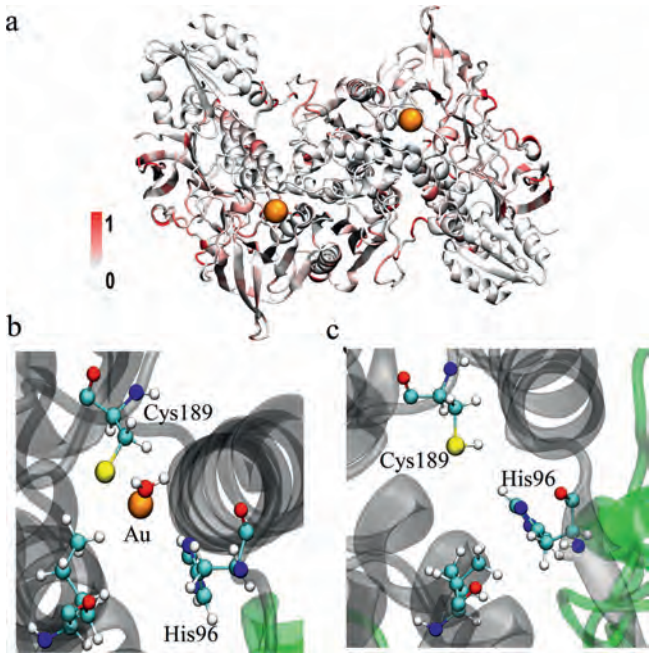

Fig. 3. Conformational analysis for Sys-1 and Sys-2. (a) Difference in RMSF between Sys-1 and Sys-2. (b) Amino acids within 5.0 Å of gold ion of Sys-1. (c) The corresponding amino acids in Sys-2. C, N, O, S, and Au atoms are displayed in gray, blue, red, yellow, and orange colors, respectively.

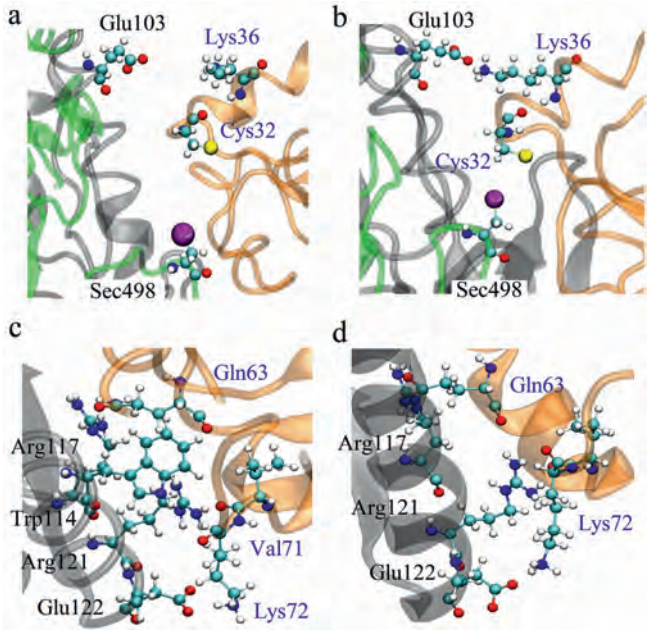

Fig. 4. The interaction between α-helix of TrxR1 and Trx for Sys-1 and Sys-2, respectively. The interaction amino acid pairs for Sys-1 (a, c) and Sys-2 (b, d). H, C, N, O and S atoms are displayed in white, gray, blue, red, and yellow colors, respectively.

applicable to the present system and can accurately describe the present process (Fig. S1 and Table S1 in Supporting information).

We calculated the root mean square fluctuation (RMSF) value in Sys-1 relative to the corresponding amino acid in Sys-2, as shown in Fig. 3a. The RMSF in the initial conformations for the two systems shows that it was slightly different overall with the maximum RMSF value of only 1.9 Å (Fig. 3a). While in the stable configurations for the two systems, the maximum RMSF value reaches 3.2 Å. The difference mainly comes from the interface between the TrxR1 enzyme and the Trx substrate, as shown in Fig. 3a.

For TrxR1/Trx monomer complex, the simulation results show that the gold ion anchors the sulfur atoms in Cys189 and is stable in the hydrophobic cavity C at the beginning of the α-helix bound to Trx. The gold ion was enclosed in a cavity composed of His96, Trp98, Ile212, and one H_2O (as shown in Fig. 3b). The corresponding amino acids in Sys-2 were shown in Fig. 3c. The distance between the sulfur atom and the gold ion in Cys189 is only 2.3 Å (Fig. S4 in Supporting information). His96 and Leu212 are also within the 5 Å range of the gold ion. These amino acids will be significantly disturbed by the gold ion, which will reduce the stability of the entire system, especially the nearby α-helix. This also explains the phenomenon that the RMSD fluctuation of Sys-1 in Fig. S2a is greater than that of Sys-2.

It is reported that the interface of the TrxR1/Trx complex is quite small [17], involving only residues 31–74 in Trx and 103–146 in TrxR1, which are susceptible to ion interference and destruction. In order to explore the mechanism by which the gold ion affect the activity of TrxR1, we first calculated the average interaction energy between the α-helix of TrxR1 and the substrate Trx after the Sys-1 and Sys-2 systems were stabilized during 90–120 ns. The interaction energy of the Sys-1 was lower with 52.05 kcal/mol than that of Sys-2 (Fig. S3 in Supporting information), indicating the Sys-1 system binds more stable than Sys-2. Based on the stable binding structure of Sys-1, the introduction of the gold ion increases the distance between Trx and the upper α helix (deviation from the C-terminal redox center), but enhances the hydrogen bond interaction between Trx and the lower α helix. In other words, Trx prefers to bind to the "wrong" site deviated from the C-terminal redox site, although the binding strength is enhanced by the introduction of the gold ion. In the dimer system composed of TrxR1/Trx, the N-terminal redox center (Cys59/Cys64) obtains electrons from NADPH and transfers them to the C-terminal redox center of another monomer (Cys498/Sec498), and finally reduces the substrate Trx. The transfer of electrons from TrxR1 to Trx was an essential part of the TrxR1 catalytic process. In this process, Sec498 obtains electrons near the N-terminal redox site, and then stretches to the solvent to transfer the electrons to the substrate Trx. The minimum distance between the reduction site of Sec498 and Trx is less than 5.0 Å, which can complete the electron transfer process. We counted the distance between the C terminal redox site (Se atom of Sec498) of TrxR1 and the active site (S atom of Cys32) of Trx substrate in the range of 90–120 ns simulation. The average distance was 8.9 and 4.0 Å for Sys-1 and Sys-2 (Fig. S2b in Supporting information), respectively, indicating that the TrxR1 catalysing process cannot be completed in Sys-1.

Molecular dynamics simulation data provides more structural details of the interaction between the α-helix of TrxR1 and Trx. The TrxR1 and Trx were mainly combined through the interaction of Glu103, Trp114, Arg121, Glu122 in TrxR1 and Lys36, Gln63, Val71, Lys72 in Trx. Because the α-helix is too long to analyze the structural details, it is artificially divided into upper and lower regions. The upper half mainly contains the weak interaction (hydrogen bond and salt bridge) between Glu103 of TrxR1 and Lys36 of Trx, as well as the interaction between the C-terminal redox center of TrxR1 and the Trx redox center (Fig. 4a). As shown in Figs. 4a and b, there is no interaction between Glu103 and Lys36 for Sys-1, while there is a hydrogen bond and an ionic bond between them in Sys-2. The average distance was 7.3 Å and 2.6 Å between Glu103 and Lys36 for Sys-1 and Sys-2, respectively (Figs. S5a and b in Supporting information). Similarly, Sec498 (which belongs to the C terminal redox region) of Sys-2 has a hydrogen bond with Cys32 (which belongs to the Trx substrate), but no hydrogen bond is formed between two amino acids in Sys-1 (Figs. 4a and b). The distance between Sec498 and Cys32 was 4.0 Å for Sys-2 and such

gap allow electron transfer from TrxR1 to Trx, while that in Sys-1 was 8.9 Å thus the electron could not transfer from TrxR1 to Trx. Glu103-Lys36 and Sec498-Cys32, for Sys-1 (Fig. 4a) and Sys-2 (Fig. 4b). The lower part is the main part of the interaction between TrxR1 and the Trx (Figs. 4c and d). The weakly interacting amino acids are in this region except Glu103 of TrxR1 and Lys36 of Trx. By comparing Sys-1 with Sys-2, it can be found that the hydrogen bond interactions between Arg117-Gln63 and Arg121-Glu71 in Sys-1 are formed (Figs. S5c and d in Supporting information). The distances between these amino acids and the gold ion are much farer than 15.0 Å, and they are unlikely to be directly affected by the gold ion. However, the side chain of arginine is relatively long and can be easily disturbed. In any case, the amino acids closer to the gold ion are more affected from the view of spatial position, revealing the correlation between the gold ion and them.

From the structural detail analysis, the gold ion anchoring on Cys189 can be stabilized in the nearby hydrophobic cavity. At the same time, it will destroy the weak interaction between Glu103 and Lys36, and changed the binding conformation between the α-helix and the substrate Trx. This is not conducive to the accurate combination of TrxR1 and Trx, and destroys the process of Sec498 in TrxR1 transmitting electrons to the substrate Trx, thereby affecting the activity of TrxR1.

In a summary, we synthesized a type of gold clusters that can significantly inhibit the activity of TrxR1 in tumor cells, and then explored the potential enzyme activity inhibition mechanism. The gold ion anchoring Cys189 exists stably in the cage composed of His96, Trp98, Leu212 and one H_2O. The introduction of the gold ion increases the distance between Glu103 in the α-helix of TrxR1 and Lys63 in Trx, destroying the hydrogen bond and salt bridge interaction between them. This significantly increase the distance between Sec498 in TrxR1 and Cys32 in Trx, disrupting the electron transfer from Sec498 to Cys32, thereby inhibiting the activity of TrxR1, named as electron transfer destroying approach. Our illustration is very different from the previously generally recognized that gold clusters will directly bind to Sec498 thus inhibit TrxR1 activity.

Declaration of competing interest

The authors declare that they have no known competing financial interests or personal relationships that could have appeared to influence the work reported in this paper.

Acknowledgments

This work was financially supported by the National Science Foundation of China (Nos. 21727817, U2067214, 11621505, 31971311) and the National Key Basic Research Program of China (No. 2020YFA0710700).

Supplementary materials

Supplementary material associated with this article can be found, in the online version, at doi:10.1016/j.cclet.2022.04.004.

References

[1] A. Holmgren, C. Johansson, C. Berndt, et al., Biochem. Soc. Trans. 33 (2005) 1375–1377.
[2] M. Selenius, A.K. Rundlof, E. Olm, A.P. Fernande, M. Bjornstedt, Antioxid. Redox. Sign. 12 (2010) 867–880.
[3] S. Urig, K. Fritz-Wolf, R. Réau, et al., Angew. Chem. Int. Ed. 45 (2006) 1881–1886.
[4] A. Holmgren, M. Bjornstedt, Methods Enzymol. 252 (1995) 199–208.
[5] S.J.A. Elias, Biochim. Biophys. Acta 1790 (2009) 495–526.
[6] C.H. Lillig, A. Holmgren, Antioxid. Redox. Sign. 9 (2007) 25–47.
[7] D. Wang, S.J. Lippard, Nat. Rev. Drug. Discov. 4 (2005) 307–320.
[8] E.S.J. Arnér, H. Nakamura, T. Sasada, et al., Free Radicals Biol. Med. 31 (2001) 1170–1178.
[9] J. Lu, L.V. Papp, J.G. Fang, et al., Cancer Res. 66 (2006) 4410–4418.
[10] R. Zhao, A. Holmgren, J. Biol. Chem. 277 (2002) 39456–39462.
[11] B.R. You, W.H. Park, Int. J. Oncol. 48 (2016) 2197–2204.
[12] A. Jastrzab, E. Skrzydlewska, J. Enzyme Inhib. Med. Chem. 36 (2021) 362–371.
[13] Q. Cheng, T. Sandalova, Y. Lindqvist, E.S.J. Arner, J. Biol. Chem. 284 (2009) 3998–4008.
[14] J.J. Jia, W.S. Geng, Z.Q. Wang, L. Chen, X.S. Zeng, Cancer Chemoth. Pharm. 84 (2019) 453–470.
[15] D. Parsonage, F. Sheng, K. Hirata, et al., J. Struct. Biol. 194 (2016) 180–190.
[16] F. Angelucci, A.A. Sayed, D.L. Williams, et al., J. Biol. Chem. 284 (2009) 28977–28985.
[17] K. Fritz-Wolf, S. Kehr, M. Stumpf, S. Rahlfs, K. Becker, Nat. Commun. 2 (2011) 1–8.
[18] S.W. Zeng, K.T. Yong, I. Roy, et al., Plasmonics 6 (2011) 491–506.
[19] B.Z. Zheng, L. Qian, H.Y. Yuan, et al., Talanta 82 (2010) 177–183.
[20] M.R. Hormozi-Nezhad, P. Karami, H. Robatjazi, RSC Adv. 3 (2013) 7726–7732.
[21] Q.Z. Wu, H.Q. Cao, Q.Y. Luan, et al., Inorg. Chem. 47 (2008) 5882–5888.
[22] J. Zhai, L.N. Zhao, L.N. Zheng, et al., ACS Omega 2 (2017) 276–282.
[23] R. Liu, Y.L. Wang, Q. Yuan, et al., Chem. Commun. 50 (2014) 10687–10690.
[24] X.C. Zhang, R. Liu, Q. Yuan, et al., ACS Nano 12 (2018) 11139–11151.
[25] V.H. Teixeira, A.S.C. Capacho, M. Machuqueiro, Proteins 84 (2016) 1836–1843.
[26] M. Fereidoonnezhad, H.A. Mirsadeghi, S. Abedanzadeh, et al., New J. Chem. 43 (2019) 13173–13182.
[27] R. Rubbiani, T.N. Zehnder, C. Mari, et al., ChemMedChem 9 (2014) 2781–2790.